A00-39773

AIAA 2000-4030

A GRAPHICAL METHOD FOR GRAVITY-ASSIST TRAJECTORY DESIGN

Nathan J. Strange* and James M. Longuski†

School of Aeronautics and Astronautics, Purdue University, West Lafayette, Indiana 47907-1282

We introduce a new analytical technique directly related to Tisserand's criterion, which permits us to quickly identify all viable gravity-assist sequences to a given destination from an energy standpoint. The method is best presented by a simple graphical technique. The graphical technique readily demonstrates that VEE, VEME, and VEEJ (gravity assists via Venus, Earth, and Jupiter) are tremendously effective sequences. Estimates are made for the shortest flight times for a given launch energy to each planet. This graphical technique should provide mission designers with a potent tool for finding economical gravity-assist trajectories to many targets of high scientific interest in the Solar System.

Introduction

MISSIONS to the outer Solar System and to Mercury can be expensive both in terms of launch cost and travel time. The technique of gravity assist has been key to making these targets accessible. Missions from Mariner 10 to Cassini have used gravity assists for deep space exploration.

In the 1800s, studies by Leverrier (see Broucke[1]) and Tisserand (see Roy[2]) into the perturbations of the orbits of planets and comets laid the foundation for the gravity-assist technique. In the 1950s, Battin[3] proposed using a planetary gravity assist to return a spacecraft to Earth without the use of propellant. Later, several investigators[4-7] studied the potential of gravity-assist swingby maneuvers for planetary exploration.

Well-known classical paths such as the VEEGA (Venus-Earth-Earth Gravity-Assist) trajectory that was used by the Galileo spacecraft have proved very effective. Yet, it is unclear whether or in what situations a better path might exist. Non-classical paths such as the VEME (Venus-Earth-Mars-Earth) proposed by Petropoulos et al.,[8] can sometimes exceed the VEEGA's performance.

In this paper, we use an energy-based method to investigate the potential and to establish the performance envelope of various gravity-assist paths. We develop a method to assess all patched-conic trajectory alternatives.

Approach

STOUR (Satellite Tour Design Program) is a software tool that was developed by JPL for the Galileo mission tour design.[9] This program has been enhanced and extended at Purdue to enable the automated design of gravity-assist tours in the Solar System as well as the satellite system of Jupiter.[10-13] STOUR uses the patched-conic method to calculate all gravity-assist trajectories meeting specified requirements.

Given a path, or sequence of gravity-assist bodies STOUR can step through a range of launch dates to find all gravity-assist trajectories that follow the path. The searches

* Graduate Student, Member AIAA.

† Professor, Associate Fellow AIAA.

can be computationally intense, sometimes requiring weeks of computer time for wide launch windows and multiple flyby paths.

A path of gravity-assist bodies must be specified prior to executing an STOUR run. Often the computational time required renders an exhaustive search of all possible paths infeasible. What we need is a method to identify the most promising paths prior to conducting an STOUR search. Also a method is needed to identify all viable paths. Ideally, we want a method that generates the best trajectory (in terms of low launch energy and short flight time) to a given planet for any given launch period.

Graphical Method

The "P-r_p" plot developed for the Europa Orbiter mission design[14] offers a method for selecting a ballistic path of gravity-assist bodies for computation in STOUR. This is an energy-based method similar to the Gravity Assist Potential (GAP) plots described by Petropoulos et al.[8] The P-r_p graph uses energy contours related to Tisserand's criterion (see Roy[2]) to illustrate gravity-assist trajectories.

A P-r_p plot for Venus, Earth, Mars, and Jupiter is shown in Fig. 1. This is a graph of heliocentric orbits in the ecliptic as period, P, versus periapsis, r_p. Assuming the planets are in circular, coplanar orbits, contours of constant V_∞ for each planet are drawn using patched-conic theory. A gravity assist rotates the V_∞ vector of the spacecraft along one of these contours to modify the orbit about the Sun. Each contour represents orbits with the same energy relative the given planet. A flyby of a planet may change the energy of a spacecraft relative to the Sun and other planets, but not relative to the flyby body.

The furthest point to the upper right on the V_∞ contour corresponds to positive alignment of the spacecraft's velocity vector with the planet's velocity. (This point represents the highest heliocentric energy possible for encounter with the planet. Thus, the encounter is at perihelion.) Rotation of the V_∞ vector

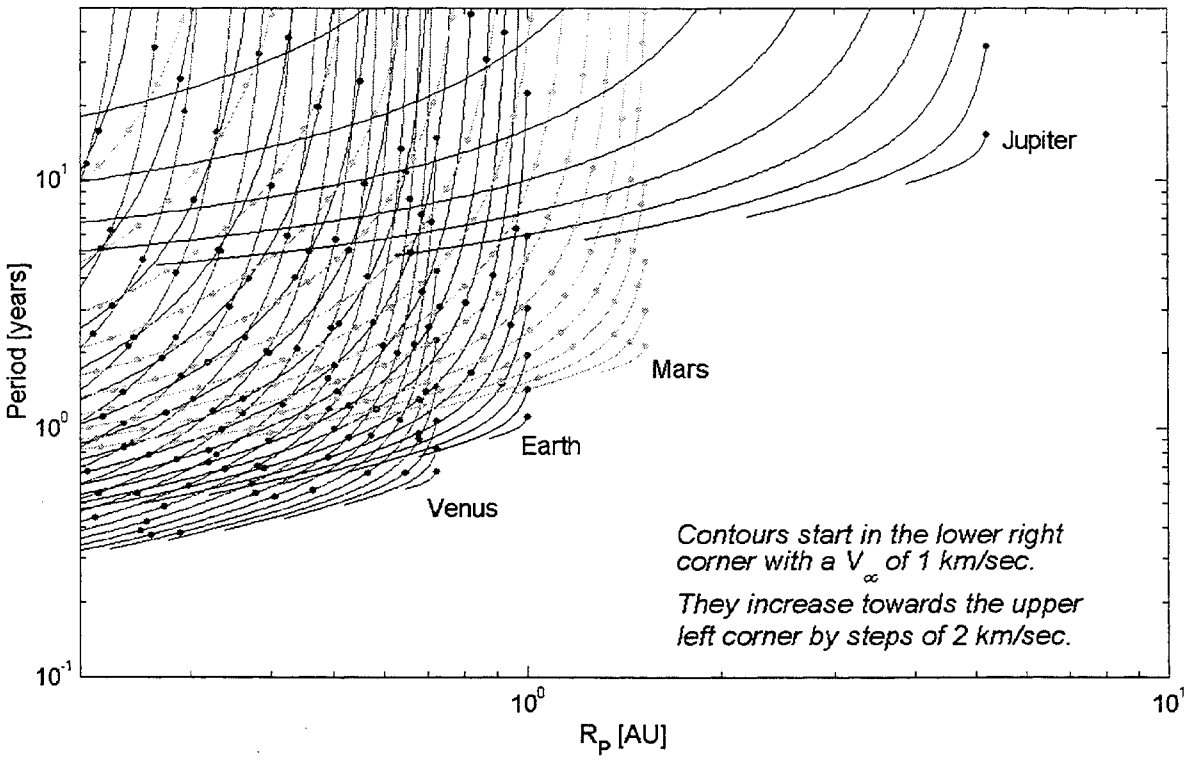

Fig. 1 P-rp plot. A single point represents an orbit about the Sun. Movement along a V_∞ contour represents the effect of a flyby. Tick marks separate 200 km flybys at Venus, Earth, and Mars, and 5 Jovian Radii flybys at Jupiter. V_∞ contours have values of 1, 3, 5, 7, etc. km/sec.

away from this alignment corresponds to moving from right to left on the V_∞ contour towards negative alignment with the planet's velocity vector. (This point corresponds to the lowest heliocentric energy, an encounter at aphelion.)

The contours in Fig. 1 start next to each planet's name at a V_∞ of 1 km/sec, then increase in steps of 2 km/sec towards the upper left of the plot. The point where contours from different planets intersect represents a potential transfer orbit between those two planets. Comparing these contours gives the values of V_∞ at each gravity-assist body for this transfer orbit. We can string together tours of different planets by connecting the contours. We use flybys to move along a contour until it intersects another contour, and then fly through the transfer orbit at the intersection of the contours to get to the next planet. This process tells us if a tour is possible from an energy standpoint, but not from a phasing (timing) point of view. (I.e. we assume that each planet is always located at the proper position for the flyby to take place.) In this way we can assess the potential performance of a tour prior to the laborious calculations by a tool such as STOUR (which does solve the phasing problem).

In Fig. 1, we constrain the flybys to have a minimum altitude of 200 km above the surface of each terrestrial planet and an altitude of 5 Jovian radii at Jupiter by limiting how far we can travel along a contour in one flyby. This is illustrated on the plot by tick marks (shown as dots on the plot). From one tick mark on a contour we may move a maximum of the distance to the next tick mark (either up or down that contour) before violating the altitude constraint. When not starting at a tick mark, the nearby tick mark spacing is used to estimate the distance.

The P-r_p plot can be used to easily find and evaluate paths for gravity-assist trajectories such as the VEEGA (Fig. 2). The VEEGA allows a low Earth launch energy (here a V_∞ of

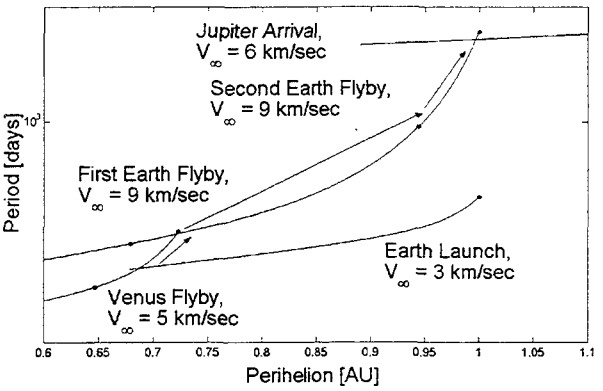

Fig. 2 Illustrating a VEEGA with a P-r_p plot (Venus-Earth-Earth Gravity Assist).

only 3 km/sec) to place a spacecraft on a Jupiter-bound trajectory. The VEEGA starts by launching into an orbit with a perihelion low enough to reach Venus. A single Venus flyby is then used to increase the spacecraft's V_∞ at Earth high enough to reach Jupiter (i.e. 9 km/sec). Two Earth flybys are then needed to rotate the spacecraft's V_∞ vector so that it reaches Jupiter. (The distance to Jupiter along Earth's V_∞ contour is greater than the tick mark spacing for one flyby.) We see that a VEEGA is effectively the same as launching from Earth with a higher energy (9 km/sec verses 3 km/sec).

In 1889, Tisserand discovered an invariant quantity that held for comets before and after perturbations of their orbit by Jupiter. He used this criterion to identify a comet with a new orbital period and perihelion as the same comet observed at an earlier date. The contours on the P-r_p also represent orbits with the same Tisserand constant. Here we are using planets to intentionally perturb the spacecraft's orbit about the Sun. Tisserand's criterion has long been used as a check of the assumptions made in designing trajectories with patched-conic analysis.[15] This invariant is given by:

$$T = r_{plan}/a + 2[a(1-e^2)/r_{plan}]^{1/2} \cos i \quad (1)$$

where r_{plan} is the distance from the Sun to the flyby planet, a is the semimajor axis of the spacecraft orbit, e is the eccentricity and i is the inclination.

A plot of period verses periapsis can only depict elliptic and circular orbits. However, if we change the y-axis from period to specific energy we get another graph that can show hyperbolic and parabolic orbits as well. This "E-r_p" plot can then represent all heliocentric orbits. Henceforth, we will formally refer to these graphs as Tisserand graphs. Since we are assuming the planets to be in circular coplaner orbits, the argument of periapsis and longitude of ascending node of the heliocentric orbit have no effect on V_∞ and flight path angle. If we wished to consider orbits outside of the ecliptic, we would need to add inclination as a third axis on these graphs, and our V_∞ contours would become surfaces.

The relative scaling of the energies and distances of the inner planets in comparison to the outer planets makes generation of one readable E-r_p plot impractical for the entire Solar System. It is more convenient to group the inner planets and outer planets separately as in Figs. 3 and 4. Figure 3 shows horizontal dash-dotted lines for the energies of orbits that are able to reach each of the outer planets. Contours that cross the line labeled "Jupiter" are able to reach Jupiter; contours that cross the next line may reach Saturn; etc. The V_∞ contours start at 1 km/sec and increase in steps of 2 km/sec towards the upper left of the plot. The tick mark spacings are for 200 km altitude flybys of the terrestrial planets.

Figure 4 shows vertical dash-dotted lines for orbits with periapses that can reach the various inner planets (Y for Mercury, V for Venus, E for Earth, and M for Mars). On this plot the V_∞ contours also start at 1 km/sec and increase towards the upper left by steps of 2 km/sec. However, the tick mark spacing is different for each planet. Jupiter's (altitude) tick marks are spaced at 5 Jovian radii to avoid radiation. Saturn's tick marks are spaced at 2 Saturnian radii to avoid the rings. Uranus's and Neptune's tick marks are spaced by one planetary radii to avoid rings as well, and Pluto's tick marks are spaced at 200 km.

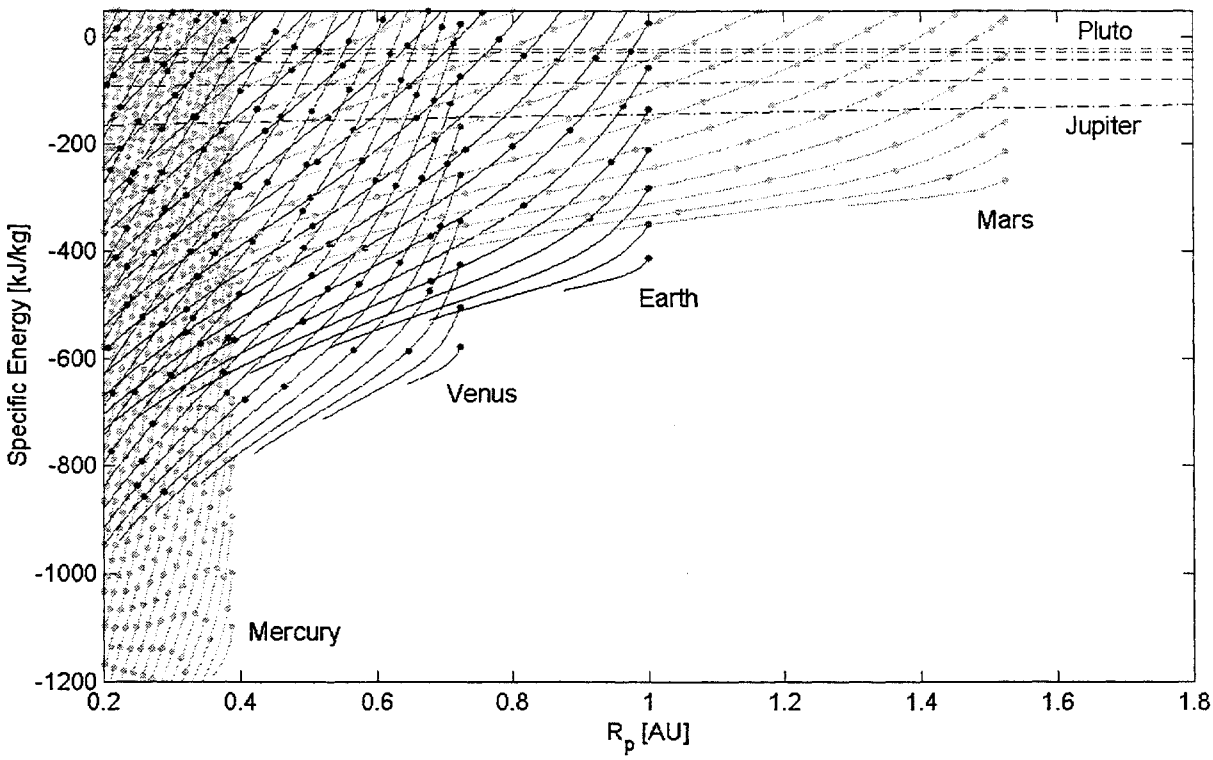

Fig. 3 E-r_p plot for the inner planets. Tick marks separate 200 km altitude flybys. V_∞ contours have values of 1, 3, 5, 7, etc. km/sec. The horizontal dash-dotted lines denote orbits that reach Jupiter, Saturn, Uranus, Neptune, and Pluto.

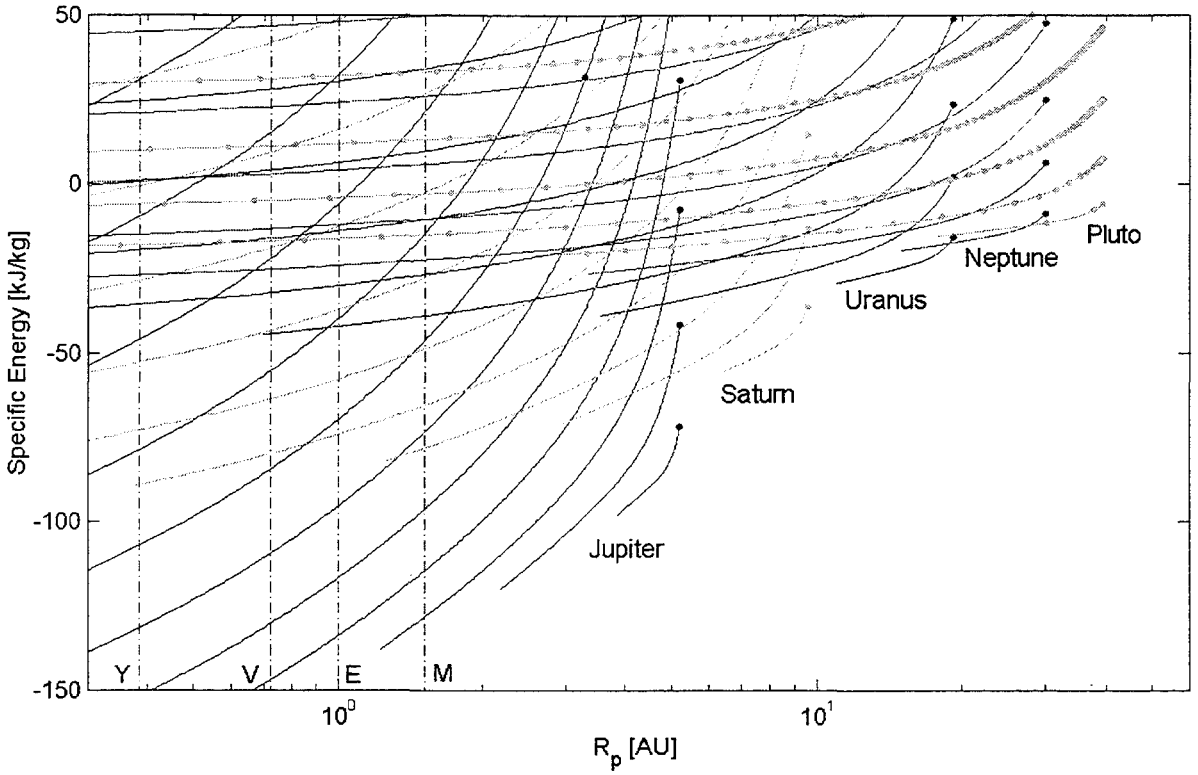

Fig. 4 E-r_p plot for the outer planets. Altitude tick marks separate flybys of 5 R_J at Jupiter, 2R_S at Saturn, 1 radii at Uranus and Neptune, and 200 km at Pluto. V_∞ contours have values of 1, 3, 5, 7, etc. km/sec. The vertical dash-dotted lines denote orbits that reach Mercury, Venus, Earth, and Mars.

Although these two plots can be combined to design tours, it is often much easier to generate a new plot with only the 4 or 5 planets of interest for the tour (such as the destination planet, Venus, Earth, Mars, and sometimes Jupiter).

Figure 5 shows a plot to design tours to Mercury with V_∞ contours incremented by steps of 2 km/sec. Two paths are shown launching from Earth with a V_∞ of 3 km/sec. One path is EVEY (Earth-Venus-Earth-Mercury) and arrives at Mercury with a V_∞ of 10 km/sec (this value is interpolated between the 9 km/sec and 11 km/sec Mercury V_∞ contours). The second path is EVEVY and arrives at 9 km/sec.

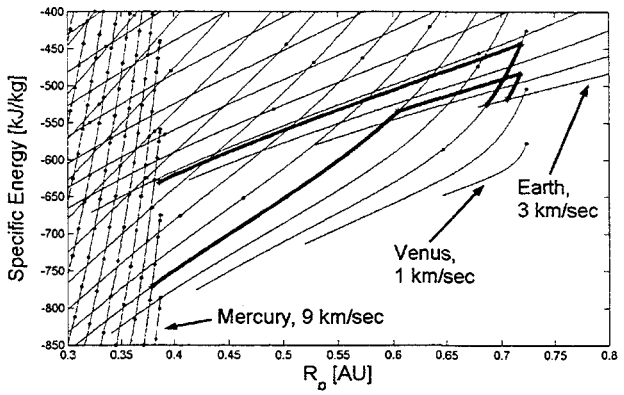

Fig. 5 Mercury E-r_p plot. V_∞ steps of 2 km/sec.

Figure 6 shows V_∞ contours for Venus, Earth, Mars and Jupiter for design of missions to the outer planets. Although the arrival V_∞ at a planet whose contours are not shown on the plot cannot be read, the value can be interpolated by remembering that lower V_∞s are toward the bottom right of the plot.

For a launch V_∞ of 3 km/sec we can identify several paths that get to Jupiter from Fig. 6: EVEEJ, EVEMEJ, EVEVEJ, EVEEMJ, EVEVVVJ, EMEMEEJ, etc. In addition, we can see that once any trajectory gets to Jupiter from Earth or Venus, it can reach any of the outer planets via a single Jupiter gravity assist.

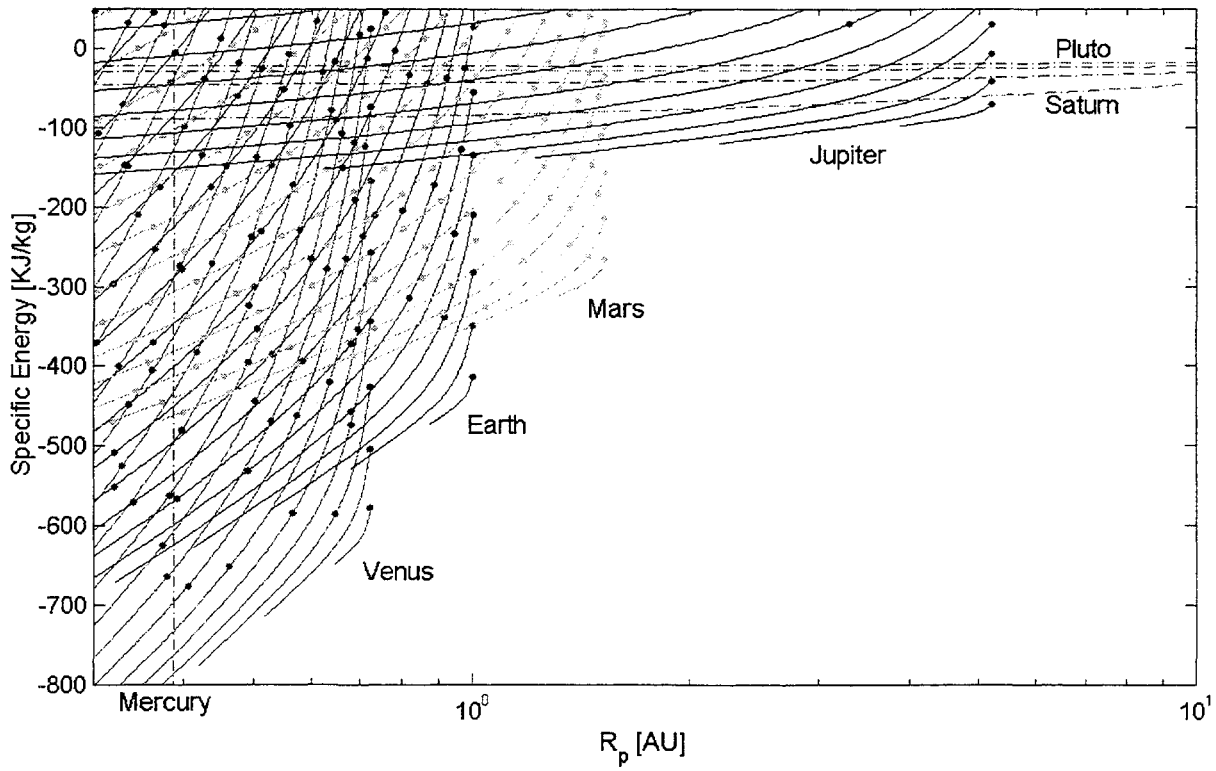

Fig. 6 E-r_p design plot. Altitude tick marks separate flybys of 5 R_J at Jupiter, and 200 km at Venus, Earth and Mars. V_∞ contours have values of 1, 3, 5, 7, etc. km/sec. The dash-dotted lines denote orbits that reach Mercury, Saturn, Uranus, Neptune, and Pluto.

If tick marks are stoplights, then Jupiter contours must be freeways.

If we start with the simplest of the Jupiter trajectories, the VEEGA, we can increase its effectiveness by adding a leveraging flyby with Mars or Venus between the two gravity assists. Although Mars has closer tick marks than Venus (i.e. it has less gravity), a leveraging flyby of Mars sends us further up an Earth V_∞ contour, enabling us to achieve a higher final heliocentric energy than with Venus as a leveraging body. We can also see cases where pumping down (i.e. decreasing heliocentric energy) at Mars gives a larger V_∞ at Venus or Earth which can get us to Jupiter when 2 or 3 Mars pump-ups (i.e. flybys that increase heliocentric energy) cannot get us to Jupiter.

By generating these plots for a specific problem, we can easily determine the minimum launch energy to fly a given path, or the minimum number of flyby bodies needed to reach a destination for a given launch energy. However, we would like to be able to compare the flight time for different paths. We would like to know if a high-energy 5-body path is faster than a lower energy 3-body path.

Flight Time

Flight time can be estimated for a tour found by the graphical method. Given the periapsis and specific energy of the transfer orbit, there is a finite set of arcs that connect the two planets on the transfer orbit. If we limit our consideration to orbits which complete less than one revolution about the Sun, there are eight arcs which connect two planets for a given periapsis and energy.

A point where two V_∞ contours intersect is an orbit that crosses the orbits of two planets. This orbit can be used to travel from the planet nearer the Sun to the planet further out, i.e. "up". It can also be used to travel from the outermost planet to the planet closer to the sun, or "down". Additionally, each of the two planetary encounters may be on either an outbound (i.e. after periapsis and before apoapsis) or an inbound (i.e. before periapsis)

leg. The eight permutations of these possibilities give rise to eight possible transfer arcs between two planets for a given specific energy and periapsis.

Figure 7 illustrates the possible transfers. An up transfer that leaves the innermost planet outbound and arrives at the second planet outbound goes from t_1 to t_2. Similarly a transfer from $-t_2$ to t_1 would be a down transfer leaving inbound and arriving outbound.

Table 1 shows the flight time for these combinations. In this table, "I-I" denotes a transfer leaving the first planet inbound and arriving at the second planet inbound, "O-I" leaves the first planet outbound and arrives at the second inbound, etc. Here P is the period of the orbit, t_1 is the time from periapsis of the orbit at the inner planet encounter and t_2 is the time for the outer planet encounter. The first two rows in the table are for elliptic arcs only, as they require flying through apoapsis.

Table 1 Flight times for possible arcs

Up	Down	Flight Time
I-I	O-O	$P + t_1 - t_2$ [a]
O-I	O-I	$P - t_1 - t_2$ [a]
I-O	I-O	$t_1 + t_2$
O-O	I-I	$t_2 - t_1$

[a] This arc is not possible for hyperbolic or parabolic orbits as it requires flying through apoapsis.

When stringing these arcs together into a tour, we must be careful that when we arrive at a planet inbound that we also leave the planet inbound and when we arrive outbound we also leave outbound. The one exception is when we are able to overturn our velocity vector to get the same heliocentric flight path angle but inbound rather than outbound or vice-versa. This happens at the far left and right ends of a V_∞ contour when we have enough turning to go all the way to the end; further turning reverses our direction of travel on the V_∞ contour. (We come back down the contour with the opposite heliocentric flight path angle.)

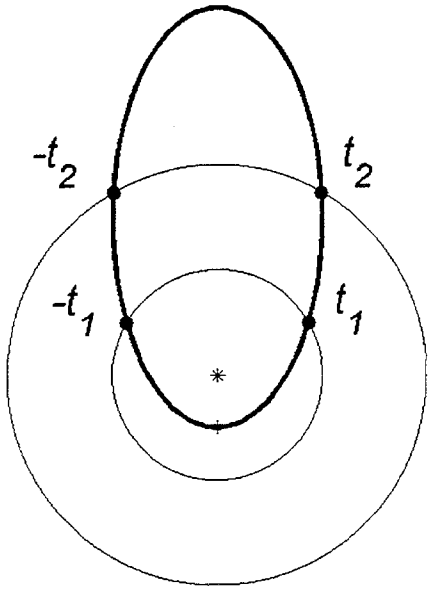

Fig. 7 Illustration of possible transfer arcs. Here t_1 is the time from periapsis of the transfer orbit to its crossing of the inner planet's orbit and t_2 is time to its crossing of the outer planet's orbit. An I-I transfer up would go from $-t_1$ to $-t_2$. An I-O transfer down would go from $-t_2$ to t_1.

The time of flight estimate is calculated by a program, which connects contours on a plot into tours. This program selects the minimum time possible to get to a given planet for a given launch energy. The phasing (timing) problem is ignored in these calculations, so the results can range from optimistic to infeasible.

Automated Traversal of E-Rp Plots

To automatically search for possible tours on an E-r_p plot, the plot is discretized. This is done by selecting a set of V_∞ contours for each planet. Where these contours intersect is a node of the grid, i.e. a possible transfer orbit for a tour. Additional nodes are added for specified resonant orbits at each planet.

A set of nodes on a launch V_∞ contour is chosen to start the traversal of the plot. A second level of nodes is comprised of all nodes that can be reached in a single flyby from the initial set of nodes. The flight time is calculated from each initial node to each node on the second level, and the fastest flight time

and the initial node for that flight time is then saved for each node on the second level. This gives the first two flyby bodies in a path.

After the fastest path to all nodes on the second level has been computed, a third level is investigated comprised of all nodes that can be reached with one flyby from the nodes on the second level. The fastest flight time to each node on the third level is saved along with the initial node and the node on the second level comprising the path to the node on the third level. This process is continued until the fastest path to every node on the grid has been computed. If from the third level or higher it is possible to reach a node on the second level faster than from the first, the faster path is used and that node is then moved up to the fourth level or higher (based on how many flybys were needed to get that low cost).

An added complexity to the process is that the actual flight time from one node to another depends on whether we encounter each planet inbound or outbound and whether we are going up or down (see Table 1). To address this, two cost functions are tracked for each node. One is the time of flight for a path whose final flyby is outbound, the other inbound.

Using this algorithm we find the fastest path to every planet on the grid for discrete V_∞s. The fastest path for a specified arrival V_∞ contour is also calculated.

For a destination planet and a launch V_∞ contour, this method predicts the fastest path to that planet from an energy point of view. The required location of the planets (i.e. the phasing required to actually fly this path) may occur rarely or never. Visual inspection of a Tisserand graph already tells us the minimum number of flyby bodies to reach a planet or if a given path can reach a planet.

This method has application beyond the design of purely ballistic trajectories. Johnson and Longuski[16] have used Tisserand graphs to assess the performance of aerogravity-assist trajectories. Future work may include the analysis of maneuvers between gravity assists such as in ΔV-EGA trajectories.

Results

Table 2 shows the potentially fastest path to each of the nine planets for launch V_∞ values of 3, 5, 7, 9, and 11 km/sec (ignoring phasing). This was generated on a grid of V_∞ contours separated by 1 km/sec. Paths were truncated after the fifth body. (When no limit on flybys was imposed 15-and 17-body paths to Pluto were found for which the needed phasing would never occur.) The lowest Hohmann V_∞ to any other planet is used as the lower bound for each planet's contours and the upper bound is set based upon the most energetic

Table 2 Potentially fastest paths (ignoring phasing)

Launch V_∞ = 3 km/sec		*Launch V_∞ = 5 km/sec*	
EVEVY	*0.8 yr.*	EVY	*0.3 yr.*
EV	*0.3 yr.*	EV	*0.2 yr.*
EVEM	*0.7 yr.*	EM	*0.3 yr.*
EVEVEJ	*2.4 yr.*	EVEVEJ	*2.1 yr.*
EVEEJS	*7.5 yr.*	EVMVES	*4.2 yr.*
EVEEJU	*13.0 yr.*	EVEMJU	*8.1 yr.*
EVEEJN	*20.0 yr.*	EVEEJN	*11.3 yr.*
EVEEJP	*27.8 yr.*	EVEEJP	*13.7 yr.*
Launch V_∞ = 7 km/sec		*Launch V_∞ = 9 km/sec*	
EVY	*0.2 yr.*	EVY	*0.2 yr.*
EV	*0.1 yr.*	EV	*0.1 yr.*
EM	*0.3 yr.*	EM	*0.2 yr.*
EMEMJ	*2.0 yr.*	EMEJ	*1.7 yr.*
EMEMJS	*3.7 yr.*	EMEJS	*3.1 yr.*
EMEMJU	*6.6 yr.*	EMEJSU	*5.5 yr.*
EMEJSN	*9.9 yr.*	EMEJSN	*7.9 yr.*
EMSJSP [a]	*12.3 yr.*	EMEJSP	*9.9 yr.*
Launch V_∞ = 11 km/sec			
EVY	*0.2 yr.*		
EV	*0.1 yr.*		
EM	*0.2 yr.*		
EMJ	*1.3 yr.*		
EMJS	*2.6 yr.*		
EMEJSU	*4.7 yr.*		
EMEJSN	*6.9 yr.*		
EMEJSP	*8.7 yr.*		

[a]This path is not possible due to the phasing of two Saturn flybys.

heliocentric hyperbola that can be created with gravity assists starting from an elliptic orbit. Resonant orbits of up to 6:1 (i.e. 6 planet revs to 1 spacecraft rev) were considered for all of the inner planets, as well as 3:2, 1:2, 1:3, and for Earth, Venus, and Mars.

Table 2 should be interpreted as a performance envelope for the flight time needed with a given launch energy. This analysis assumes that the planets are in the correct position for the best flyby (in terms of flight time) and, as such, probably underestimates the flight time required for most paths. Paths containing sequences such as VMV or MEM may never occur due to the requirement that a planet be in the proper position for a second flyby. Clearly the path EMSJSP for the launch V_∞ of 7 km/sec is infeasible for this reason.

Table 3 shows flight times to the outer planets for a sampling of paths at various launch energies. We notice that paths such as VEEGA perform very well for low launch energies but begin to offer diminishing returns as we increase launch energy to the point where an increase of launch V_∞ from 5 km/sec to 7 km/sec offers no improvement (within 0.1 year).

These tables can be used in conjunction with the Tisserand graphs to give a ballpark estimate of the flight time for different paths. However a tool such as STOUR is needed to compute realistic trajectories. Petropouplos et al.[8] found that all of these paths reach Jupiter in the span of 1999-2030 with the exception of the EVEVEE and EVEMEE paths which they did not investigate. The flight times for the actual trajectories are 1 to 3 years longer than the estimates in this table.

Conclusion

Tisserand graphs facilitate the assessment of potential gravity-assist paths. Both arrival and launch V_∞ may be studied for such a path. The graphs also make many characteristics of a possible path highly conspicuous.

This is a powerful tool, based on Tisserand's criterion, which permits us to

Table 3 Flight times for potential gravity-assist paths (ignoring phasing)

Path	Launch V_∞	Jupiter	Saturn	Uranus	Neptune	Pluto
EVE...	6 km/sec	2.3 yr.	—	—	—	—
EVEE...	3 km/sec	4.8 yr.	—	—	—	—
EVEE...	4 km/sec	3.9 yr.	6.8 yr.	13.6 yr.	—	—
EVEE...	5 km/sec	3.8 yr.	6.5 yr.	12.4 yr.	19.0 yr.	25.8 yr.
EVEE...	7 km/sec	3.8 yr.	6.5 yr.	12.4 yr.	19.0 yr.	25.8 yr.
EVVV...	6 km/sec	5.8 yr.	—	—	—	—
EVEM...	5 km/sec	2.2 yr.	—	—	—	—
EVEEM...	5 km/sec	3.8 yr.	6.3 yr.	11.9 yr.	19.5 yr.	27.5 yr.
EVEVE...	3 km/sec	2.4 yr.	—	—	—	—
EVEVE...	5 km/sec	2.1 yr.	5.0 yr.	—	—	—
EVEME...	3 km/sec	2.7 yr.	—	—	—	—
EVEME...	5 km/sec	3.3 yr.	6.7 yr.	12.0 yr.	20.2 yr.	28.2 yr.
EVEVEE...	3 km/sec	4.2 yr.	6.9 yr.	12.7 yr.	18.2 yr.	23.5 yr.
EVEMEE...	3 km/sec	4.7 yr.	8.0 yr.	14.8 yr.	—	—
Paths With Jovian Gravity Assist						
EJ...	9 km/sec		5.0 yr.	10.4 yr.	17.4 yr.	25.3 yr.
EJ...	11 km /sec		2.7 yr.	5.4 yr.	8.4 yr.	11.0 yr.
EVEJ...	6 km/sec		4.7 yr.	9.2 yr.	14.8 yr.	20.8 yr.
EVVVJ...	6 km/sec		7.9 yr.	11.7 yr.	16.0 yr.	19.5 yr.
EVEEJ...	3 km/sec		7.5 yr.	13.0 yr.	20.0 yr.	27.8 yr.
EVEEJ...	5 km/sec		5.5 yr.	8.5 yr.	11.3 yr.	13.7 yr.
EVEEJ...	9 km/sec		5.4 yr.	8.4 yr.	11.2 yr.	13.7 yr.
EVEVEJ...	3 km/sec		4.4 yr.	7.9 yr.	12.2 yr.	15.7 yr.
EVEVEJ...	5 km/sec		3.5 yr.	6.2 yr.	9.2 yr.	11.7 yr.

readily construct gravity-assist paths to any destination in the Solar System. All paths so constructed are feasible from an energy perspective. Paths that do not exist on a Tisserand graph are strictly infeasible. Thus we can eliminate unnecessary searches and confine path finding to those, which obey the criterion. Estimates of flight time can be made for a given launch V_∞, thus providing another criterion for candidate rejection. After applying these criteria, the mission designer can be assured that remaining candidate paths are worth pursuing in the laborious calculation that must follow to solve the phasing problem. This last problem is well known and discussed in great detail in the literature.

Acknowledgments

This research has been supported in part by the Jet Propulsion Laboratory, California Institute of Technology, under Contract Number 1211514 (G. T. Rosalia, Contract Manager, and Dennis V. Byrnes, Technical Manager). We thank Andrew Heaton, Wyatt Johnson, and Anastassios Petropoulos for their assistance in developing the techniques described in this paper. We also thank Dan Scheeres for pointing out the connection of our graphical technique to Tisserand's criterion. Finally, we thank Lou D'Amario, Eugene Bonfiglio, Dennis V. Byrnes, Jennie Johannesen, and Jan M. Ludwinski at JPL for their generous support, enthusiastic collaboration, and expert guidance with regard to the Europa Orbiter mission, which inspired these techniques.

References

[1]Broucke, R. A., "The Celestial Mechanics of Gravity Assist," AIAA Paper 88-4220, Aug. 1988.

[2]Roy, A. E., *Orbital Motion*, Adam Hilger, Bristol, UK, 1982, pp. 129-130.

[3]Battin, R.H., "The Determination of Round-Trip Planetary Reconnaissance Trajectories," *Journal of the Aero/Space Sciences*, Vol. 26, no. 9, Sept. 1959, pp. 545-567.

[4]Sedov, L. I., "Orbits of Cosmic Rockets Toward the Moon," *ARS Journal*, Vol. 30, No. 1, Jan 1960.

[5]Deerwester, J. M., "Jupiter Swingby Missions to the Outer Planets," *Journal of Spacecraft and Rockets*, Vol. 3, No. 10, Oct. 1966, pp. 1564-1567.

[6]Flandro, G. A., "Fast Reconnaissance Missions to the Outer Solar System Utilizing Energy Derived from the Gravitational Filed of Jupiter," *Astronautica Acta*, Vol. 12, No. 4, 1966. pp. 329-337.

[7]Farquhar, R., and Stern, S. A., "Pushing Back the Frontier: A Mission to the Pluto-Charon System," *Planetary Report*, Vol. 10, No 4, 1990, pp. 18-23.

[8]Petropoulos, A. E, Longuski, J. M., and Bonfiglio, E. P., "Trajectories to Jupiter via Gravity Assists from Venus, Earth, and Mars," AIAA Paper 98-4284, Aug. 1998. Also, to appear in *Journal of Spacecraft and Rockets*.

[9]Rinderle, E. A., "Galileo User's Guide, Mission Design System, Satellite Tour Analysis and Design Subsystem," Jet Propulsion Laboratory, California Institute of Technology, Pasadena, CA, JPL D-263, 1986.

[10]Williams, S. N., "Automated Design of Multiple Encounter Gravity-Assist Trajectories," Master's Thesis, School of Aeronautics and Astronautics, Purdue University, West Lafayette, IN, Aug.1990.

[11]Longuski, J. M. and Williams, S. N., "Automated Design of Gravity-Assist Trajectories to Mars and the Outer Planets," *Celestial Mechanics and Dynamical Astronomy*, Vol. 52, No. 3, 1991, pp. 207-220.

[12]Patel, M. R., "Automated Design of Delta-V Gravity-Assist Trajectories for Solar System Exploration," Master's Thesis, School of Aeronautics and Astronautics, Purdue University, West Lafayette, IN, Aug.1993.

[13]Bonfiglio, E. P., "Automated Design of Gravity-Assist and Aerogravity-Assist Trajectories" Master's Thesis, School of Aeronautics and Astronautics, Purdue University, West Lafayette, IN, Aug.1999.

[14]Heaton, A. F., Strange, N. J., Longuski, J. M., and Bonfiglio, E. B. "Automated Design of the Europa Orbiter Tour," AIAA Paper 2000-4034, Aug. 2000.

[15]Szebehely, V., *Theory of Orbits: The Restricted Problem of Three Bodies*, Academic Press, New York, 1967, pp. 586-587.

[16]Johnson, W. R. and Longuski, J. M., "Design of Aerogravity-Assist Trajectories," AIAA Paper 2000-4031, Aug. 2000.